CHEMISTRY

Reactivity of prehydrated electrons toward nucleobases and nucleotides in aqueous solution

Jun Ma,[1] Furong Wang,[1] Sergey A. Denisov,[1] Amitava Adhikary,[2] Mehran Mostafavi[1]*

DNA damage induced via dissociative attachment by low-energy electrons (0 to 20 eV) is well studied in both gas and condensed phases. However, the reactivity of ultrashort-lived prehydrated electrons (e_{pre}^-) with DNA components in a biologically relevant environment has not been fully explored to date. The electron transfer processes of e_{pre}^- to the DNA nucleobases G, A, C, and T and to nucleosides/nucleotides were investigated by using 7-ps electron pulse radiolysis coupled with pump-probe transient absorption spectroscopy in aqueous solutions. In contrast to previous results, obtained by using femtosecond laser pump-probe spectroscopy, we show that G and A cannot scavenge e_{pre}^- at concentrations of ≤ 50 mM. Observation of a substantial decrease of the initial yield of hydrated electrons (e_{hyd}^-) and formation of nucleobase/nucleotide anion radicals at increasing nucleobase/nucleotide concentrations present direct evidence for the earliest step in reductive DNA damage by ionizing radiation. Our results show that e_{pre}^- is more reactive with pyrimidine than purine nucleobases/nucleotides with a reactivity order of T > C > A > G. In addition, analyses of transient signals show that the signal due to formation of the resulting anion radical directly correlates with the loss of the initial e_{hyd}^- signal. Therefore, our results do not agree with the previously proposed dissociation of transient negative ions in nucleobase/nucleotide solutions within the timescale of these experiments. Moreover, in a molecularly crowded medium (for example, in the presence of 6 M phosphate), the scavenging efficiency of e_{pre}^- by G is significantly enhanced. This finding implies that reductive DNA damage by ionizing radiation depends on the microenvironment around e_{pre}^-.

INTRODUCTION

Water makes up about 70% of biological systems, and most ionizing radiation is initially absorbed by water surrounding the biomolecules. This results in radiation damage of biomolecules via the quasi-direct as well as by the indirect effects of radiation (1, 2). Strand breaks, an important DNA damage that may be lethal to cells, occur in higher abundance in hydrated DNA than in dry DNA (2). In water radiolysis, a secondary electron with a high kinetic energy (E_c) is ejected, thereby leaving a hole [water cation radical ($H_2O^{\bullet+}$)] behind in the nanometer-size volumes along the radiation tracks. In a subpicosecond range, $H_2O^{\bullet+}$ is transformed into hydroxyl radical ($^{\bullet}OH$) via proton transfer to a proximate water molecule (3, 4). The secondary electrons cause further ionizations, leading to a cascade of electrons with lower kinetic energies. After losing their kinetic energy via ionization and excitation events, the electron is thermalized and undergoes a multistep hydration process with a time constant of ca. ≤ 1 ps, becoming fully trapped as a hydrated or solvated electron (e_{hyd}^-) (3). Before complete solvation (or hydration), the electron exists in its presolvated (or prehydrated) state (e_{pre}^-) with a small or no kinetic energy. Here, for clarity, we use the term "prehydrated electrons" to account for the precursors of the e_{hyd}^- with excess energy (fig. S1) (3).

The oxidative pathway of DNA damage is induced by $^{\bullet}OH$ attack via the indirect effect and by the direct-type (direct + quasi-direct) effects of ionizing radiation; it has been suggested that the oxidative pathway is the dominant pathway for strand break formation (1, 2, 5–7). In addition, over the last decade, tremendous efforts have been made to unravel the role of energetic electrons, especially of low-energy electrons (LEEs; 0 to 20 eV) in the reductive pathway of DNA damage. Sanche and coworkers (8) provided the first experimental observation of DNA strand cleavage induced by LEEs. This work led to numerous

mechanistic studies on LEE-induced damage in naked DNA models including DNA building blocks in gas phase or condensed states, single- and double-stranded oligomers of defined sequences, plasmid DNA, and cellular DNA (9, 10). These studies established that, initially, LEEs lead to the formation of resonant transient negative ions (TNIs) in DNA models. Subsequent fragmentations of these TNIs occur via the dissociative electron attachment (DEA) process (11). Experiments, including LEE scattering (12), photoelectron imaging (13), and Rydberg electron transfer spectroscopy (14), along with theoretical calculations (15–20) have shed new light on the interaction of excess electrons with hydrated DNA subunits and on the formation of TNIs.

e_{pre}^- and e_{hyd}^- in water are considered to be the states of electrons in biological systems rather than the states of electrons in the gas phase. Investigations of the fast one-electron reductions of biomolecules (for example, nucleobases and nucleosides/nucleotides) by e_{pre}^- in competition with its hydration process are a subject of experimental challenge (3, 21). From the existing literatures (2, 15, 16, 21), it is conceivable that scavenging of e_{pre}^- by purine and pyrimidine nucleobases in aqueous medium could be the initial step for the reaction of e_{pre}^-. This reaction leads to the formation of TNI, that is, the transient nucleobase anion radical. Subsequently, this TNI leads to the generation of the complex DNA damage (2, 3, 15, 16). Therefore, it is important to examine the rates and extents of reactions of DNA building blocks with e_{pre}^-. The nature of short-lived transient species (that is, the TNIs), which are produced immediately after the electron capture, needs to be clarified for a better understanding of the DNA bond cleavage induced by e_{pre}^-. In the following paragraph, we describe the work by Wang et al. (22), who, by using a femtosecond laser pump-probe technique with single-wavelength absorption detection in the ultraviolet (UV) region, claimed to have observed the real-time fast electron addition of e_{pre}^- to particular nucleobases and nucleotides. According to the authors, these studies did provide the evidence of TNI formation of nucleobases (22).

In 50 mM guanine (G) and thymine (T) systems, the anion radicals, which were labeled as the TNIs of nucleobases, evolve from two-photon

[1]Laboratoire de Chimie Physique, CNRS–Université Paris-Sud 11, Bâtiment 349, 91405 Orsay, France. [2]Department of Chemistry, Oakland University, 146 Library Drive, Rochester, MI 48309, USA.
*Corresponding author. Email: mehran.mostafavi@u-psud.fr

(318 nm) ionization; the authors suggested that the TNIs of nucleobases decayed within a few tens of picoseconds (22). However, neither the absorption spectra in the visible and near-infrared regions nor the kinetics of e_{hyd}^- and e_{pre}^- were reported by these authors. We believe that these parameters are crucial to verify the presence of e_{hyd}^- and e_{pre}^- in the UV region. In addition, the pump and probe wavelengths are very close in the UV region and thus could be affected by optical artifacts. Thus, the results reported by Wang *et al.* (22) can be called into question. The time-resolved radiolysis technique with a high-energy electron pulse has advantages over the femtosecond laser pump-probe spectroscopy to study the effect of radiation in liquids (3, 4, 21, 23, 24), although laser-based setups have better time resolution. Here, we have used the picosecond (7 ps) electron pulse (7 MeV) radiolysis coupled with UV-visible (UV-Vis) transient absorption spectroscopy to explore the reactivity of e_{pre}^- with nucleobases (X), nucleosides, and 5′-nucleotides (XMP). On the basis of our previous work (21) that showed increased lifetimes of e_{pre}^- in a crowded medium (6 M phosphate), we conducted pulse radiolysis studies on the reactions of e_{pre}^- with nucleobases/nucleotides in 6 M phosphate. Our results and conclusions reported in this work disagree with those reported by Wang *et al.* (22).

The rationale of our work is that the e_{pre}^- interaction with nucleobases can be investigated by measuring the initial yield of e_{hyd}^- formation. This is achieved by using picosecond electron pulse radiolysis as an alternative approach to femtosecond laser photolysis (3, 21, 23–25). The e_{hyd}^- displays a broad absorption band showing a maximum at 715 nm with a relatively high extinction coefficient under ambient conditions and thus can be detected with precision. When the precursor of e_{hyd}^- (that is, e_{pre}^-) reacts with nucleobase molecules in competition to its solvation dynamics, the yield of formation of e_{hyd}^- in solutions of nucleobases/nucleotides will decrease in comparison to that of e_{hyd}^- in water. The laser-triggered continuous probe light of our pulse radiolysis system has the advantage that it covers a broad spectral range from 380 to 1500 nm. This allows us to determine yields and transient spectra of the resulting intermediates using the 7-ps electron pulse.

RESULTS AND DISCUSSION

As shown in Fig. 1, in contrast to the results reported by Wang *et al.* (22), after a 7-ps electron pulse, the initial absorbance that correlates with the radiolytic yield of e_{hyd}^- in neat water was not affected by adding G up to its maximum solubility of 50 mM in 90 mM NaOH at 22.5°C. The fact that the TNI of G did not form in these conditions indicates that all precursors of e_{hyd}^- exclusively undergo the solvation dynamics as it happens in neat water, forming e_{hyd}^- in less than 1 ps. Higher concentrations of solute, with the consequent smaller reaction radius, would need to be present to increase the probability of e_{pre}^- trapping by e_{pre}^- scavengers in aqueous solution (26).

We note that the electron tunneling mechanism of long-range interaction could not be excluded because of the large delocalization radius of excess electrons in water (24, 27) and because of the available empty π* orbitals of nucleobases. However, these results point out that these long-range interactions of e_{pre}^- are not significant in these diluted solutions (≤50 mM). Our results also show that the decay of e_{hyd}^- in the presence of G molecules is similar to that of e_{hyd}^- in neat water (Fig. 1) within the time range of 200 ps. Furthermore, in basic conditions (pH ~ 12), G is deprotonated, and its reaction rate constant with e_{hyd}^- is relatively low (2×10^9 M^{-1} s^{-1}) (1, 28); thus, a decay of e_{hyd}^- is not apparent in this time scale.
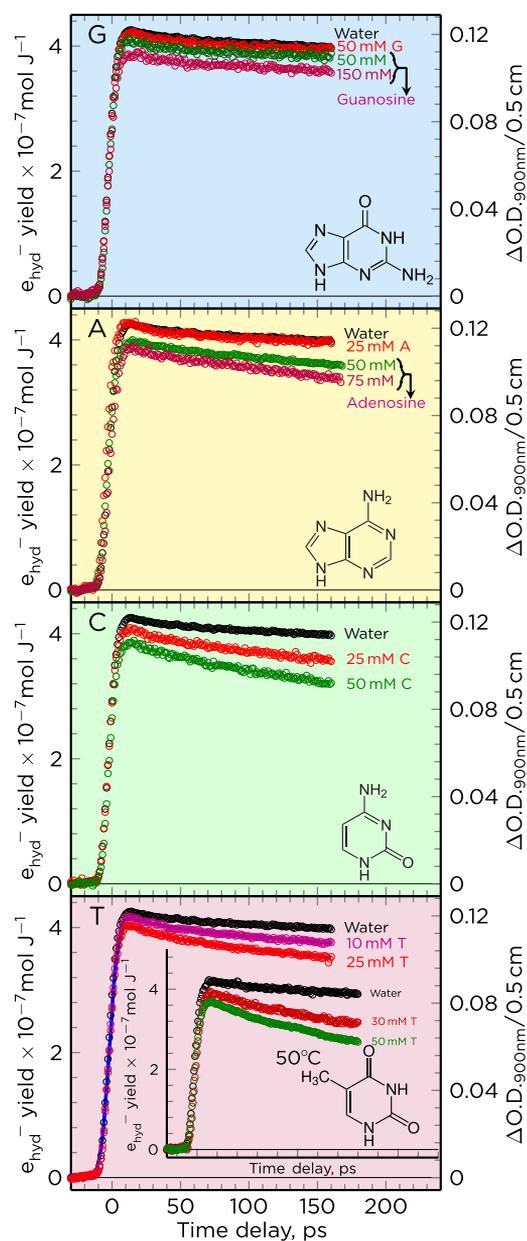

Fig. 1. Transient absorption kinetic traces of e_{hyd}^- in liquid water containing G, A, C, and T compounds with different concentrations (10 to 150 mM). To increase the solubilities of purine nucleobases, the solutions were prepared in 90 mM NaOH followed by the work of Wang *et al.* (22). Radiolytic yields of e_{hyd}^- are shown in the left axes, and these correspond to the absorbance in the right axes. The dose per electron pulse was 55.3 grays (Gy). The radiolytic yield of e_{hyd}^- is not affected even in 50 mM G solution within 1% uncertainty. The solid line is the theoretical fit; we have obtained it using time-dependent rate constants. ΔO.D.$_{900nm}$, optical density at 900 nm.

To increase the solute concentration up to 150 mM and to shorten the distance between electrons and reactants, we replaced the G nucleobase by the nucleoside, guanosine (Guo). We note here that the ribose itself is a much less efficient site than the G nucleobase for trapping electrons (the rate constant of the reaction of e_{hyd}^- with ribose, <10^7 M^{-1} s^{-1}) (28, 29). The presence of Guo at 150 mM does not change the e_{hyd}^- absorption band.

A decrease of the initial yield of e_{hyd}^- in the presence of Guo becomes detectable between 50 and 150 mM [~3% at 50 mM and ~8%

at 150 mM (Fig. 1)]. Two factors explain these observations: (i) Guanosine has a larger molecular size that leads to a shorter distance between the reactants, and (ii) density functional theory (DFT) calculations of electron attachment to nucleosides showed that the addition of the deoxyribose moiety promotes electron scavenging because of higher electron affinity values of the nucleosides (15–20, 30). These results provide the first estimate of the extent of the involvement of e^-_{pre} in fast electron attachment to nucleobases, leading to the formation of the TNI (that is, $G^{*\bullet-}$ or $G^{\bullet-}$). However, the detection of this species is challenging due to its low yield and weak absorption.

Extensive experimental and theoretical determination of gas-phase electron affinities of canonical nucleobases have been carried out (15–20, 30). These results show that the gas-phase vertical electron affinities of all DNA nucleobases are negative; the adiabatic electron affinity of T and cytosine (C) are near 0 eV, and those of purines are negative (15, 17, 30). However, the solvation has a pronounced effect on the binding of an electron with nucleobases. One can assume that the electron affinity of a nucleobase in its fully hydrated form is associated with its efficiency of e^-_{pre} capture. Calculations using DFT by Sevilla and coworkers (30) pointed out that the adiabatic electron affinity of all DNA nucleobases increases substantially with the solvent in comparison to the gas phase.

Therefore, the extension of our measurements to various DNA nucleobases will be helpful for evaluating the influence of solvent on the electron affinities of nucleobases/nucleotides. The results with different nucleobases can be seen in Fig. 1. It is observed in Fig. 1 that, similar to G, 25 to 50 mM adenine (A) did not react with e^-_{pre}. However, the initial yield of e^-_{hyd} was found to be lower in the presence of 75 mM A compared to that in the presence of G. Thus, we conclude that A showed a slightly higher capability of trapping e^-_{pre} and e^-_{hyd} than G. We also observed a decrease of e^-_{hyd} yield in T and C solutions at 25 mM. The relative ratios of e^-_{hyd} yield in T and C solutions with respect to water are determined to be ~0.93 and ~0.97, respectively. Because the solubility of T is limited at room temperature (maximum solubility of T at room temperature in water is ~25 mM), we performed similar measurements at 50°C. The decrease of the initial yield of e^-_{hyd} was more pronounced (Fig. 1, inset).

The reactivity of e^-_{pre} with the four nucleobases is T > C > A > G. Nucleotide solutions show the same order. These results are presented in Fig. 2. Among the nucleotides, guanosine 5′-monophosphate (GMP) shows the lowest reactivity toward e^-_{pre} (only 7% of the electrons are scavenged), whereas thymidine 5′-monophosphate (TMP) has the highest efficiency with 40% of the nonequilibrium electrons being scavenged. Following the procedure developed by Jonah et al. (26) to determine the reaction rate constant of e^-_{pre} with a given solute, we were able to roughly estimate the reaction rates of e^-_{pre} with nucleotides as ~5 × 10^{12} M^{-1} s^{-1} for TMP, 4 × 10^{12} M^{-1} s^{-1} for cytidine 5′-monophosphate (CMP), 3 × 10^{12} M^{-1} s^{-1} for adenosine 5′-monophosphate (AMP), and 0.6 × 10^{12} M^{-1} s^{-1} GMP. These rate constant values do agree well with those for near-conduction band electrons in nonpolar solvents (24, 27). More accurate determination of these rates requires a broader range of XMP concentrations; however, this is limited by XMP solubility in water (26).

The decrease of the initial yield of e^-_{hyd} formation presents the evidence for the e^-_{pre} reaction with DNA nucleobases and nucleotides. This chemical reaction is completed within the subpicosecond range and can be regarded as the earliest efficient indirect damage event. The decay of e^-_{hyd} is accelerated by raising the concentration of T and C. The rate constants of the reaction of e^-_{hyd} with these two nucleobases
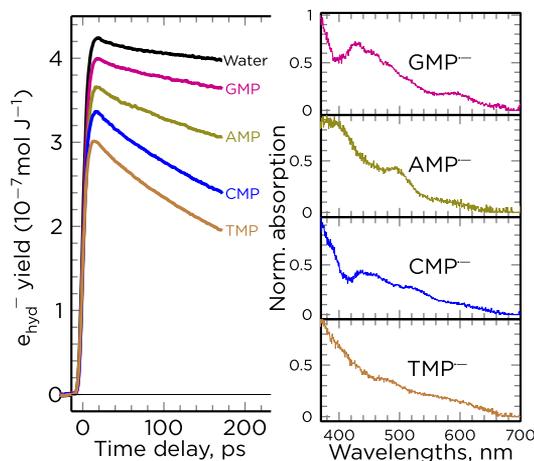

Fig. 2. Transient absorption spectra of the nucleotide anion radicals (GMP$^{\bullet-}$, AMP$^{\bullet-}$, CMP$^{\bullet-}$, and TMP$^{\bullet-}$ or the TNIs of nucleotides) observed at 7 ps (right) and the kinetics of e^-_{hyd} in the presence of 250 mM nucleotides in water (left). We have obtained the spectra of absorbing radicals via subtraction of the appropriate extent of the absorption spectrum of e^-_{hyd} from the original experimentally recorded two-dimensional (2D) spectrum using global data analysis.

were determined to be as high as 1.4 × 10^{10} M^{-1} s^{-1} under ambient conditions, which agrees well with the corresponding values in the literature (29). As expected, the decay of e^-_{hyd} is faster at 50°C, and the value of the rate constant is found to be around 3.2 × 10^{10} M^{-1} s^{-1}.

Recently, the existence of surface-bound electrons in liquid water having a binding energy of −1.6 eV proposed by Abel and coworkers (31) has been a matter of debate. These authors experimentally measured the vertical detachment energy of e^-_{hyd} as −3.3 eV (fig. S1) and proposed that e^-_{hyd} may not able to reduce the DNA/RNA because it is beyond the electron attachment window. However, this reaction was suggested to occur between those electrons and the DNA/RNA molecules located at the interface. This view is in contrast to the ab initio molecular dynamics simulations by Kumar et al. (32) and a number of pulse radiolysis studies on the reaction of e^-_{hyd} with DNA models (1, 28). The accurately calculated standard redox potentials of nucleobases and e^-_{hyd} predict the extent of the reaction of e^-_{hyd} with nucleobases (32), which is in excellent agreement with our observations using solutions of nucleobases. Meanwhile, it should be argued here that the decrease of e^-_{hyd} signal within the electron pulse (7 ps) is not due to the fast reaction of e^-_{hyd} because we have calculated the time-dependent rate constants for T (Fig. 1). In agreement with the work of Jonah et al. (26), the reaction of e^-_{hyd} during the 7-ps pulse is less than 1% of the total, which justifies that the decrease of the e^-_{hyd} signal within the electron pulse is primarily due to the reaction of e^-_{pre} with nucleobases and nucleosides/nucleotides.

Identification of the sites at which electrons are initially trapped in DNA to produce the anion radicals is an important question to elucidate the pathways of reductive DNA damage. This question directly relates to the subsequent charge transfer and bond dissociations. The electron spin resonance studies by Bernhard (33) and Wang and Sevilla (34) concluded that pyrimidines have a higher electron affinity than purines. Steenken and Jovanovic (35) found that T has the highest reduction potential, whereas G has the lowest. The conclusions of the work carried out by Wang and Sevilla (34) along with those obtained using pulse radiolysis studies (1, 28, 35) state that among the nucleobase anion radicals, G anion radical ($G^{\bullet-}$) undergoes very fast protonation in oligomers containing only G. However, this reaction

does not occur in double-stranded DNA owing to the fast electron transfer from G$^{\bullet-}$ to C and T forming the C and T anion radicals (C$^{\bullet-}$ and T$^{\bullet-}$, respectively). Our results presented in Fig. 1 and, more clearly, in Fig. 2 show that the loss of e_{pre}^- supports the experimental and theoretical model that the fully solvated pyrimidine nucleobases have a higher electron affinity than purines. Meanwhile, C is found to be less reactive with e_{pre}^- than T. Furthermore, our results show that A in adenosine is a better trap for e_{pre}^- than G in Guo because the initial yield of e_{hyd}^- is lower at the same nucleoside concentration.

The intrinsic higher solubility of nucleotides with respect to nucleobases in water enabled us to investigate the trapping of e_{pre}^- and e_{hyd}^- at higher concentrations of nucleobases. This gave rise to a higher yield and a better detection of spectral intermediates. As presented in Fig. 2, for 250 mM XMP solutions, global analyses of the original transient absorption matrix data (wavelength versus delay time; figs. S2 to S6) show that, besides the typical broad absorption band of e_{hyd}^-, there is one additional absorbing species that is observed in the time scale from 10 to 100 ps (figs. S7 to S10). Because the protonation of anion radical process cannot occur within the picosecond time scale, the transient species formed within the 7-ps electron pulse (Fig. 2, right) is assigned to the nucleotide anion radical (XMP$^{\bullet-}$). This assignment is based on the fact that the spectrum observed is almost identical with the previously reported anion radical spectra obtained by nanosecond pulse radiolysis via the reaction of e_{hyd}^- with nucleotides (36, 37). Because the reaction of e_{hyd}^- with nucleotides also takes place, we observed a slight increase of the rate of formation of the nucleotide anion radicals over tens of picoseconds (Fig. 3 and figs. S7 to S10). This suggests that the reactions of both e_{pre}^- and e_{hyd}^- with nucleotides essentially lead to the same transient anion radical XMP$^{\bullet-}$.

In the case of AMP, the spectrum is slightly different from the reported spectrum for AMP$^{\bullet-}$ (1, 28, 35–37). It is known that, because of stacking interaction, the aqueous solution of 250 mM AMP exhibits a wide aggregation number with a distribution centered at 10 (38). Therefore, this difference might be explained by the significant AMP aggregation under our experimental conditions, inducing changes in the absorption spectrum.

The work of Wang et al. (22) suggested that dissociation is the dominant process in G and T nucleotide anion radicals in the proportion of 60 and 36%, respectively. In our work, by taking the established molar absorption coefficient of the XMP$^{\bullet-}$ in the literature (37), the yield of formation of XMP$^{\bullet-}$ is carefully deduced from the kinetics via global analysis. For instance, in the case of G, the maximal value of the extinction coefficient of e_{hyd}^- and GMP$^{\bullet-}$ in the UV-Vis spectral window were

19,045 M^{-1} cm^{-1} at 700 nm and 4200 ± 100 M^{-1} cm^{-1} at 380 nm. As shown in Fig. 3, the formation yield of GMP$^{\bullet-}$ at 7 ps is calculated to be $2.5 \pm 0.5 \times 10^{-8}$ mol J^{-1}. The quantity of electrons being captured by the GMP molecules in competition with the hydration of electrons is marked by the initial yield difference of e_{hyd}^- in the presence and absence of GMP. Unexpectedly, the yields of these two species are found to be nearly equal to each other. From 10 to 100 ps, there is a continuous increase of the anion radical yield due to the occurrence of a reaction of e_{hyd}^- (Fig. 3) in neutral solution. For the other three nucleotides, the results are found to be similar to those of the G system. Thus, contrary to the work by Wang et al. (22), our work establishes that the nucleotide anion radicals do not undergo dissociation.

Considering the reaction of the e_{pre}^- with nucleotides in competition with its hydration (Fig. 4), our results establish that e_{pre}^- initially attaches to the π* orbitals of nucleotides and form the TNI or excited anion radical XMP*$^{\bullet-}$. This species can either rapidly dissociate to an energetically accessible radical with a lifetime of several picoseconds or relax to form the stable anion radical XMP$^{\bullet-}$. If the dissociation of XMP*$^{\bullet-}$ does occur, then the yield of XMP$^{\bullet-}$ is expected to be lower than the electron loss. Therefore, the above analyses reveal that within the experimental error, almost all the electrons participate in the formation of XMP$^{\bullet-}$. Thus, we conclude that the dissociation pathway of XMP*$^{\bullet-}$ is not likely to occur or, at least, is not an evident process in this condition. However, it is well established that e_{hyd}^- has several precursor states during the hydration process (39, 40). Because the hydration process of the electron competes with the electron scavenging (Fig. 4), the excess energy of the electron before its full hydration can be important. The faster (shorter time) the electron scavenging, the more energy the electron has to excite the solute. We could not exclude the possibility that the DEA turns out to be more effective in a realistic environment in which the higher energy state of e_{pre}^- might be trapped by nucleobase sites. It is certainly a matter of great interest and significance and will be the subject of our further study.

To extend these studies in cellular DNA and chromatin, two important aspects need to be considered: (i) The local cellular environment surrounding the DNA is complex, including a considerable amount of other species, including proteins and inorganic salts, etc., which definitively alter the hydration process and reactivity of e_{pre}^- compared to that in neat water or in dilute solutions (41). (ii) Direct energy deposition in the hydration layer of DNA creates H$_2$O$^{\bullet+}$ and an electron located in close contact with a nucleobase. This promotes the overlap of electron and that of nucleobase wave functions in competition with charge localization on water molecules. Taking these into account, we introduced a molecularly crowded environment by selecting solutions with a high concentration of phosphate groups. As an example, we used a solution of 6 M H$_3$PO$_4$ and focused on the G case, because it showed the lowest electron scavenging efficiency. In our previous works (21, 25), it was pointed out that the concentration of H$_3$PO$_4$ effectively defines the solvation dynamics of the electron. The use of 6 M H$_3$PO$_4$
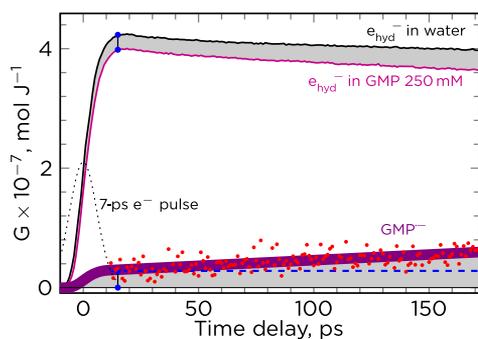

Fig. 3. The comparison of yield of the formation of GMP anion radical (GMP$^{\bullet-}$) with that of e_{pre}^- trapped by the GMP molecule before the hydration is complete. The filled gray areas represent the changes of the total yield of anion radicals from that of trapped electrons evolving with the delay time up to 170 ps.
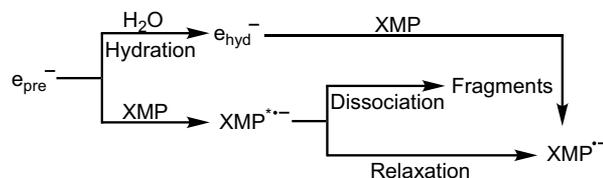

Fig. 4. Scheme representing the reactivity of e_{pre}^- and e_{hyd}^- with XMP and possible pathways of the decay of the excited anion radical XMP*$^{\bullet-}$ (TNI).

was chosen for several reasons. In 6 M H_3PO_4, as expected from the experimentally and theoretically obtained pK_a (where K_a is the acid dissociation constant) values, G is present in its fully protonated form (for example, at N7, N9, and N1) (42). Furthermore, H_3PO_4 increases the solubility of G, which allowed us to use higher G concentrations. In 6 M H_3PO_4, the solvation of e_{pre}^- slows down significantly, thereby increasing the time for the solute to react with e_{pre}^-. However, at H_3PO_4 concentrations of >10 M, the yield of formation of e_{hyd}^- is significantly reduced due to the scavenging of its precursor, e_{pre}^-, by H_3O^+. Moreover, in 6 M H_3PO_4, the ratio between phosphate and water molecules is 6.3, which closely represents the local environment of hydrated DNA because, according to the literature (43), there are six hydration sites per phosphate group in a nucleotide. Before the time-resolved measurements, we examined the chemical stability of G in H_3PO_4 with the aid of steady-state UV-Vis absorption spectroscopy. No evidence of G decomposition during the time course of the experiment was observed.

In these acidic conditions, H_3O^+ reacts rapidly with e_{pre}^-, resulting in a reduction of e_{hyd}^- yield to 2.6×10^{-7} mol J^{-1} (Fig. 5) in comparison to the expected e_{hyd}^- yield of ca. 6×10^{-7} mol J^{-1} (1, 3, 4). Because a part of the radiation energy is deposited on the phosphate groups, the direct ionization produces a non-negligible amount of $H_2PO_4^\bullet$. For these reasons, the absorbance of e_{hyd}^- in 6 M H_3PO_4 without G was used as a reference.

As mentioned above, the steady-state UV-Vis spectral measurements show that G is fully protonated in 6 M H_3PO_4. For protonated G in 6 M H_3PO_4, we observed a significant decrease in the initial yield of e_{hyd}^- formation with respect to that obtained in the absence of H_3PO_4. For a solution containing 50 mM G, an 11% drop is found, and each increase of G concentration by 25 mM led to a corresponding decrease of e_{hyd}^- formation yield by 10%. These results established that in solutions containing phosphate, the scavenging of e_{pre}^- is notably enhanced, thereby leading to an efficient reduction of protonated G. This system with high-efficiency electron scavenging allows us to observe the formation of products, as shown in Fig. 5. The original spectrum consists of the spectral contributions from three absorbing species, e_{hyd}^-, $H_2PO_4^\bullet$, and a new transient species. Because G molecules are protonated owing to the acid medium, this spectral intermediate is assigned to the protonated G anion radical $G(H^+)^{\bullet-}$ (37). On the basis of the kinetics of $G(H^+)^{\bullet-}$, no evidence was found

for the fragmentation of the TNIs even if an appreciable amount of e_{pre}^- is captured compared to that in the dilute medium.

To conclude our discussion on the trapping of e_{pre}^- by G, we have to mention that in highly concentrated ionic solutions, e_{pre}^- forms the so-called encounter pairs. This could induce a blue shift of spectrum of both e_{hyd}^- and e_{pre}^- [for example, the absorption spectrum of e_{hyd}^- with a maximum at 650 nm, as seen in Fig. 5, whereas in water, the corresponding maximum is 715 nm (vide supra)] and thus affect the initial absorbance at certain wavelength as it was very recently found on the reactivity of e_{pre}^- and e_{hyd}^- in acids (23, 25). This important spectral change was not considered in previous investigations (24, 27) studying the reactivity of e_{pre}^-. Gauduel et al. (44) showed that e_{pre}^- forms the ion pairs with H_3O^+, denoted as (e_{pre}^-, H_3O^+), during its solvation process, within 1 ps, accompanied by a blue shift of ca. 300 nm, because the charge of excess electrons are screened by H_3O^+ ions. Moreover, in our recent work, we showed that the reactivity of the pair is different from that of e_{hyd}^- with H_3O^+, because e_{pre}^- with H_3O^+ efficiently reduces silver ions in highly concentrated acidic solutions in comparison to e_{hyd}^- (45).

The scavenging of e_{pre}^- by G in the highly concentrated H_3PO_4 can be explained by the fact that the hydration process of radiation-produced electrons is slowed relative to that in neat water. Slow hydration of the electrons is likely to occur because fewer H_2O molecules are present in a close vicinity to that electron. Consequently, the competitive reaction of e_{pre}^- with G becomes more effective. It is also difficult to rule out the possibility that both the energy of e_{pre}^- and the electron affinity of G molecules that are fully protonated in 6 M H_3PO_4 are altered in highly concentrated H_3PO_4 solutions. In addition, our results suggest that the driving force of this reaction is larger because G must remain protonated before electron addition. However, the reactivity of transient e_{pre}^- adducts (TNIs) is similar to that in water. Depending on the preexisting traps in the local hydration shell of DNA and energies of the excess electrons, the reactivity of electrons could be different. It is reported in the literature (11) that the water-ice monolayer surface enhances the dissociative attachment of ~0 eV electrons to some organic molecules. In contrast, using a molecular beam to control the hydration level of nucleobases, Kočišek et al. (46) recently showed that the presence of a few water molecules suppresses the dissociative channel by LEE (0 to 3 eV). In agreement with the abovementioned experimental result, recent molecular dynamics simulations showed that in solution, the excess electron in the vicinity of a nucleotide is rapidly (15 fs) localized on the nucleobases (18–20). In aqueous medium, our results suggested for the first time that the reactivity of e_{pre}^- could be significantly enhanced in the presence of a large quantity of ions (for example, $H_5P_2O_8^-$) and molecules (for example, H_3PO_4) other than water.
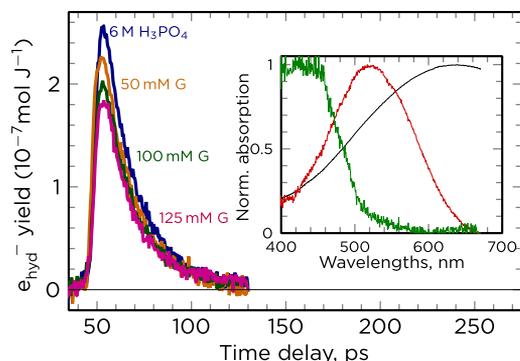

Fig. 5. Transient absorption kinetics of e_{hyd}^- in the absence (blue curve) and in the presence of different concentrations of G in 6 M H_3PO_4 solutions replacing the neat water as a medium. The normalized transient spectra consist of three absorbing species, e_{hyd}^- (black), $H_2PO_4^\bullet$ (red), and the protonated G nucleobase anion radical $G(H^+)^{\bullet-}$ (blue), produced within the electron pulse.

CONCLUSIONS
Our results establish that scavenging of e_{pre}^- by DNA nucleobases is not very efficient at moderate DNA nucleobase concentrations (≤50 mM). In particular, in the cases of G and A, capture of e_{pre}^- does not occur. However, our results show that by slowing the hydration (or solvation) process of the electron in the presence of a high concentration of phosphate, it is possible for G to efficiently scavenge the e_{pre}^- even at a low concentration (50 mM). Pyrimidine nucleobases are found to be more effective electron scavengers, with a decreasing reactivity order of T > C > A > G. Our findings disagree with those measurements performed by Wang et al. (22). However,

our results partially agree with those obtained, as early as the 1970s, by Hunt and coworkers (47). They pointed out that the effective collisions of e_{pre}^- with amino acids and mononucleotides depend on the solute concentration and solution pH. Our results also demonstrate that the spectra of nucleotide anion radicals formed by e_{pre}^- trapping can be observed at 7 ps for the first time. By comparing the initial yield of formation of electrons with the quantity of electrons scavenged during their hydration, our results suggest that the dissociation pathway of TNIs (either $X^{*\bullet-}$ or $XMP^{*\bullet-}$) does not occur in the conditions of our experiments. Thus, our radiation chemical studies predict that neither e_{pre}^- nor e_{hyd}^- can induce direct dissociation of the DNA nucleobases via the DEA pathway. Moreover, our results demonstrate that the reaction of a nucleotide with e_{pre}^- and e_{hyd}^- in neutral solutions essentially gives rise to the same anion radicals. Therefore, our study provides experimental benchmarks for theoretical calculations on the reactions of e_{pre}^- and e_{hyd}^- with DNA models. Ongoing efforts to investigate the fast electron transfer reactions in the TNIs of defined sequences of single- or double-stranded DNA oligomers and to achieve the direct observation of the subsequent fragmentation of the TNIs or stable anion radicals are under way in our laboratories.

MATERIALS AND METHODS

The picosecond pulse radiolysis transient absorbance measurements were performed at the electron facility ELYSE (Université Paris Sud) (48). The transient absorption pulse-probe setup was based on the laser-electron intrinsic synchronization resulting from the laser-triggered photocathode of the accelerator. For the present study, a broadband probe detection scheme was used, the principle of which has already been described (48). A supercontinuum, generated by focusing ~1 μJ of the laser source into a 6-mm-thick CaF_2 disk, was used as the optical probe covering a broad spectral range (380 to 1500 nm). A reference signal was split off from the broadband probe before the fused silica optical flow cell. Each of the probe and reference beams was coupled into the optical fibers, transmitted to a spectrometer, and dispersed onto a charge-coupled device. The combination of the broadband probe and the multichannel detector allowed the entire transient spectrum to be recorded in one shot; as a result, the transient spectrum was independent of the shot-to-shot fluctuations and possible long-term drifts of the electron source. For data acquisition, we cautiously maintained the same radiation dose (55.3 ± 0.5 Gy) per electron pulse that was deposited on the samples to minimize the absorbance fluctuation. All measurements were performed using a fused silica flow cell with a 5-mm optical path collinear to the electron pulse propagation. The electron pulses were ~4 nC, with an electron energy of 6 to 8 MeV, delivered at a repetition frequency of 10 Hz. The measurements were performed at 22.5°C, and for T, the measurements were performed at 22.5° and 50°C.

The experimental data matrices were analyzed by a multivariate curve resolution alternating least squares (MCR-ALS) approach. The number of the absorbing species in a data matrix was assessed by a singular value decomposition of the matrix, and an MCR-ALS analysis with the corresponding number of species was performed. Positivity constraints were imposed for both spectra and kinetics, and, when necessary, spectrum shape was also imposed (49).

The chemical compounds (nucleobases and nucleosides/nucleotides; purity, >99%) were purchased from Sigma-Aldrich and were used without further purification. To introduce a simplified molecular environment, buffer solutions were not used, and the solutions, with a typical 100-ml volume, were prepared simply by dissolving nucleobases and nucleotides in neat water. Water for dilution was purified by passage through a Millipore purification system. For only G and A nucleobases, we used 90 mM NaOH solutions to increase their solubility. The crowded molecular environment was introduced by dissolving G in 6 M H_3PO_4 solutions. UV-Vis spectroscopy was applied to examine the chemical stability of G in acid medium.

SUPPLEMENTARY MATERIALS

Supplementary material for this article is available at http://advances.sciencemag.org/cgi/content/full/3/12/e1701669/DC1

fig. S1. Schematic diagram representing the energetic cycle for the adiabatic electron solvation and its reaction with a DNA nucleobase.
fig. S2. Time-resolved 2D transient absorption map of irradiated neat water.
fig. S3. Time-resolved 2D transient absorption map of the irradiated solution of GMP at 250 mM.
fig. S4. Time-resolved 2D transient absorption map of the irradiated solution of AMP at 250 mM.
fig. S5. Time-resolved 2D transient absorption map of the irradiated solution of CMP at 250 mM.
fig. S6. Time-resolved 2D transient absorption map of the irradiated solution of TMP at 250 mM.
fig. S7. Time-dependent population and normalized spectra of hydrated electron and GMP radical anions.
fig. S8. Time-dependent population and normalized spectra of hydrated electron and TMP radical anions.
fig. S9. Time-dependent signal population and normalized spectra of hydrated electron and CMP radical anions.
fig. S10. Time-dependent population and normalized spectra of hydrated electron and AMP radical anions.

REFERENCES AND NOTES

1. C. von Sonntag, *Free-Radical-Induced DNA Damage and Its Repair: A Chemical Perspective* (Springer Berlin Heidelberg, 2009).
2. A. Adhikary, D. Becker, M. D. Sevilla, in *Applications of EPR in Radiation Research*, A. Lund, M. Shiotani, Eds. (Springer International Publishing, 2014), pp. 299–352.
3. M. D. Sevilla, D. Becker, A. Kumar, A. Adhikary, Gamma and ion-beam irradiation of DNA: Free radical mechanisms, electron effects, and radiation chemical track structure. *Radiat. Phys. Chem.* **128**, 60–74 (2016).
4. J. Ma, J. A. LaVerne, M. Mostafavi, Scavenging the water cation in concentrated acidic solutions. *J. Phys. Chem. A* **119**, 10629–10636 (2015).
5. C. Chatgilialoglu, M. D'Angelantonio, G. Kciuk, K. Bobrowski, New insights into the reaction paths of hydroxyl radicals with 2′-deoxyguanosine. *Chem. Res. Toxicol.* **24**, 2200–2206 (2011).
6. A. Adhikary, A. Kumar, S. A. Munafo, D. Khanduri, M. D. Sevilla, Prototropic equilibria in DNA containing one-electron oxidized GC: Intra-duplex vs. duplex to solvent deprotonation. *Phys. Chem. Chem. Phys.* **12**, 5353–5368 (2010).
7. P. López-Tarifa, M.-P. Gaigeot, R. Vuilleumier, I. Tavernelli, M. Alcamí, F. Martín, M.-A. Hervé du Penhoat, M.-F. Politis, Ultrafast damage following radiation-induced oxidation of uracil in aqueous solution. *Angew. Chem. Int. Ed. Engl.* **52**, 3160–3163 (2013).
8. B. Boudaïffa, P. Cloutier, D. Hunting, M. A. Huels, L. Sanche, Resonant formation of DNA strand breaks by low-energy (3 to 20 eV) electrons. *Science* **287**, 1658–1660 (2000).
9. F. Martin, P. D. Burrow, Z. Cai, P. Cloutier, D. Hunting, L. Sanche, DNA strand breaks induced by 0–4 eV electrons: The role of shape resonances. *Phys. Rev. Lett.* **93**, 068101 (2004).
10. S. K. Sahbani, L. Sanche, P. Cloutier, A. D. Bass, D. J. Hunting, Loss of cellular transformation efficiency induced by DNA irradiation with low-energy (10 eV) electrons. *J. Phys. Chem. B* **118**, 13123–13131 (2014).
11. E. Alizadeh, L. Sanche, Precursors of solvated electrons in radiobiological physics and chemistry. *Chem. Rev.* **112**, 5578–5602 (2012).
12. S. Ptasinska, S. Denifl, P. Scheier, E. Illenberger, T. D. Märk, Bond- and site-selective loss of H atoms from nucleobases by very-low-energy electrons (<3 eV). *Angew. Chem. Int. Ed. Engl.* **44**, 6941–6943 (2005).
13. M. A. Yandell, S. B. King, D. M. Neumark, Time-resolved radiation chemistry: Photoelectron imaging of transient negative ions of nucleobases. *J. Am. Chem. Soc.* **135**, 2128–2131 (2013).

14. C. Desfrançois, H. Abdoul-Carime, J. P. Schermann, Electron attachment to isolated nucleic acid bases. *J. Chem. Phys.* **104**, 7792–7794 (1996).

15. A. Kumar, M. D. Sevilla, in *Handbook of Computational Chemistry*, M. K. Shukla, J. Leszczynski, Eds. (Springer-Verlag, 2012), pp. 1215–1256.

16. J. Gu, J. Leszczynski, H. F. Schaefer III, Interactions of electrons with bare and hydrated biomolecules: From nucleic acid bases to DNA segments. *Chem. Rev.* **112**, 5603–5640 (2012).

17. K. Aflatooni, G. A. Gallup, P. D. Burrow, Electron attachment energies of the DNA bases. *J. Phys. Chem. A* **102**, 6205–6207 (1998).

18. M. Smyth, J. Kohanoff, Excess electron localization in solvated DNA bases. *Phys. Rev. Lett.* **106**, 238108 (2011).

19. M. Smyth, J. Kohanoff, Excess electron interactions with solvated DNA nucleotides: Strand breaks possible at room temperature. *J. Am. Chem. Soc.* **134**, 9122–9125 (2012).

20. M. McAllister, M. Smyth, B. Gu, G. A. Tribello, J. Kohanoff, Understanding the interaction between low-energy electrons and DNA nucleotides in aqueous solution. *J. Phys. Chem. Lett.* **6**, 3091–3097 (2015).

21. J. Ma, U. Schmidhammer, M. Mostafavi, Picosecond pulse radiolysis of highly concentrated phosphoric acid solutions: Mechanism of phosphate radical formation. *J. Phys. Chem. B.* **119**, 7180–7185 (2015).

22. C.-R. Wang, J. Nguyen, Q.-B. Lu, Bond breaks of nucleotides by dissociative electron transfer of nonequilibrium prehydrated electrons: A new molecular mechanism for reductive DNA damage. *J. Am. Chem. Soc.* **131**, 11320–11322 (2009).

23. J. Ma, U. Schmidhammer, M. Mostafavi, Direct evidence for transient pair formation between a solvated electron and H_3O^+ observed by picosecond pulse radiolysis. *J. Phys. Chem. Lett.* **5**, 2219–2223 (2014).

24. M. Mostafavi, I. Lampre, in *Recent Trends in Radiation Chemistry*, J. F. Wishart, BSM Rao, Eds. (World Scientific Publishing Company, 2010), pp. 21–58.

25. J. Ma, U. Schmidhammer, P. Pernot, M. Mostafavi, Reactivity of the strongest oxidizing species in aqueous solutions: The short-lived radical cation $H_2O^{•+}$. *J. Phys. Chem. Lett.* **5**, 258–261 (2014).

26. C. D. Jonah, J. R. Miller, M. S. Matheson, The reaction of the precursor of the hydrated electron with electron scavengers. *J. Phys. Chem.* **81**, 1618–1622 (1977).

27. I. A. Shkrob, in *Recent Trends in Radiation Chemistry* (World Scientific Publishing Company, 2010), pp. 59–96.

28. S. Steenken, Purine bases, nucleosides, and nucleotides: Aqueous solution redox chemistry and transformation reactions of their radical cations and e⁻ and OH adducts. *Chem. Rev.* **89**, 503–520 (1989).

29. G. V. Buxton, C. L. Greenstock, W. P. Helman, A. B. Ross, Critical review of rate constants for reactions of hydrated electrons, hydrogen atoms and hydroxyl radicals (˙OH/˙O⁻) in aqueous solution. *J. Phys. Chem. Ref. Data* **17**, 513–886 (1988).

30. X. Li, Z. Cai, M. D. Sevilla, DFT calculations of the electron affinities of nucleic acid bases: Dealing with negative electron affinities. *J. Phys. Chem. A* **106**, 1596–1603 (2002).

31. K. R. Siefermann, Y. Liu, E. Lugovoy, O. Link, M. Faubel, U. Buck, B. Winter, B. Abel, Binding energies, lifetimes and implications of bulk and interface solvated electrons in water. *Nat. Chem.* **2**, 274–279 (2010).

32. A. Kumar, A. Adhikary, L. Shamoun, M. D. Sevilla, Do solvated electrons (e_{aq}^-) reduce DNA bases? A Gaussian 4 and density functional theory-molecular dynamics study. *J. Phys. Chem. B.* **120**, 2115–2123 (2016).

33. W. A. Bernhard, Sites of electron trapping in DNA as determined by ESR of one-electron-reduced oligonucleotides. *J. Phys. Chem.* **93**, 2187–2189 (1989).

34. W. Wang, M. D. Sevilla, Protonation of nucleobase anions in gamma-irradiated DNA and model systems. Which DNA base is the ultimate sink for the electron? *Radiat. Res.* **138**, 9–17 (1994).

35. S. Steenken, S. V. Jovanovic, How easily oxidizable is DNA? One-electron reduction potentials of adenosine and guanosine radicals in aqueous solution. *J. Am. Chem. Soc.* **119**, 617–618 (1997).

36. L. P. Candeias, P. Wolf, P. O'Neill, S. Steenken, Reaction of hydrated electrons with guanine nucleosides: Fast protonation on carbon of the electron adduct. *J. Phys. Chem.* **96**, 10302–10307 (1992).

37. R. Yamagami, K. Kobayashi, S. Tagawa, Formation of spectral intermediate G–C and A–T anion complex in duplex DNA studied by pulse radiolysis. *J. Am. Chem. Soc.* **130**, 14772–14777 (2008).

38. R. Rymdén, P. Stilbs, Nucleotide aggregation in aqueous solution. A multicomponent self-diffusion study. *Biophys. Chem.* **21**, 145–156 (1985).

39. A. Migus, Y. Gauduel, J. L. Martin, A. Antonetti, Excess electrons in liquid water: First evidence of a prehydrated state with femtosecond lifetime. *Phys. Rev. Lett.* **58**, 1559–1562 (1987).

40. M. H. Elkins, H. L. Williams, A. T. Shreve, D. M. Neumark, Relaxation mechanism of the hydrated electron. *Science* **342**, 1496–1499 (2013).

41. H. Nikjoo, P. O'Neill, D. T. Goodhead, M. Terrisol, Computational modelling of low-energy electron-induced DNA damage by early physical and chemical events. *Int. J. Radiat. Biol.* **71**, 467–483 (1997).

42. Y. H. Jang, W. A. Goddard III, K. T. Noyes, L. C. Sowers, S. Hwang, D. S. Chung, pK_a values of guanine in water: Density functional theory calculations combined with Poisson-Boltzmann continuum-solvation model. *J. Phys. Chem. B* **107**, 344–357 (2003).

43. B. Schneider, K. Patel, H. M. Berman, Hydration of the phosphate group in double-helical DNA. *Biophys. J.* **75**, 2422–2434 (1998).

44. Y. Gauduel, S. Pommeret, A. Migus, N. Yamada, A. Antonetti, Femtosecond spectroscopy of an encounter pair radical ($H_3O^+ \cdots e^-$)$_{hyd}$ in concentrated aqueous solution. *J. Am. Chem. Soc.* **112**, 2925–2931 (1990).

45. A. Balcerzyk, U. Schmidhammer, F. Wang, A. de la Lande, M. Mostafavi, Ultrafast scavenging of the precursor of H˙ atom, (e^-, H_3O^+), in aqueous solutions. *J. Phys. Chem. B.* **120**, 9060–9066 (2016).

46. J. Kočišek, A. Pysanenko, M. Fárník, J. Fedor, Microhydration prevents fragmentation of uracil and thymine by low-energy electrons. *J. Phys. Chem. Lett.* **7**, 3401–3405 (2016).

47. J. E. Aldrich, K. Y. Lam, P. C. Shragge, J. W. Hunt, Fast electron reactions in concentrated solutions of amino acids and nucleotides. *Radiat. Res.* **63**, 42–52 (1975).

48. J. Belloni, H. Monard, F. Gobert, J.-P. Larbre, A. Demarque, V. De Waele, I. Lampre, J.-L. Marignier, M. Mostafavi, J. C. Bourdon, M. Bernard, H. Borie, T. Garvey, B. Jacquemard, B. Leblond, P. Lepercq, M. Omeich, M. Roch, J. Rodier, R. Roux, ELYSE—A picosecond electron accelerator for pulse radiolysis research. *Nucl. Instrum. Methods Phys. Res. A* **539**, 527–539 (2005).

49. C. Ruckebusch, M. Sliwa, P. Pernot, A. de Juan, R. Tauler, Comprehensive data analysis of femtosecond transient absorption spectra: A review. *J. Photochem. Photobiol. C* **13**, 1–27 (2012).

Science Advances

Reactivity of prehydrated electrons toward nucleobases and nucleotides in aqueous solution

Jun Ma, Furong Wang, Sergey A. Denisov, Amitava Adhikary and Mehran Mostafavi